

SPACE CHARGE LIMITATIONS FOR BUNCH COMPRESSION IN SYNCHROTRONS

Y.S. Yuan*, O. Boine-Frankenheim, I. Hofmann, TU Darmstadt, Germany
 G. Franchetti, GSI Helmholtzzentrum für Schwerionenforschung GmbH, Darmstadt, Germany

Abstract

Bunch compression achieved via a fast bunch rotation in longitudinal phase space is a well-accepted scheme to generate short, intense ion bunches for various applications. During bunch compression, coherent beam instabilities and incoherent single particle resonances can occur because of increasing space charge, resulting in an important limitation for the bunch intensity. We present an analysis of the relevant space charge driven beam instability and resonance phenomena during bunch compression. A coupled longitudinal-transverse envelope approach is compared with Particle-In-Cell (PIC) simulations. Two distinct cases of crossing are discussed and applied to the GSI SIS18 heavy-ion synchrotron. It is shown that during bunch compression, the 90° condition of phase advance is associated with a fourth order single particle resonance and the 120° condition with the recently discovered dispersion-induced instability. The agreement between the envelope and PIC results indicates that the stop band is defined by the 120° dispersion instability, which should be avoided during bunch compression.

INTRODUCTION

Short and intense ion or proton bunches are required for many applications, such as the production and subsequent storage of exotic nuclei or antiprotons [1], generation of dense plasmas and spallation neutron sources. Short bunches can be obtained by longitudinal rf bunch compression just before extraction from a synchrotron. Space charge represents an important limitation for the maximum compression ratio as the increasing transverse space charge tune spread leads to resonance crossing and corresponding emittance growth. Therefore, the bunch compression process must be completed as fast as possible in order to minimize the dwelling time of bunches in the extreme space charge regime.

The present study investigates bunch dynamics during compression for parameters of the SIS-18. Based on the coupled longitudinal-transverse envelope equations and PIC simulations, the intensity limitation during bunch compression related to the coherent beam instability: envelope instability [2] and dispersion-induced instability [3], and incoherent single particle resonance (fourth-order resonance) are analyzed in detail.

* yuan@temf.tu-darmstadt.de

APPROACHES FOR BUNCH COMPRESSION STUDIES

Coupled Longitudinal-Transverse Envelope System

The longitudinal envelope equation [4] can be used to describe the longitudinal beam dynamics and calculate the required rf voltage in bunch compression. By including the space-charge modified dispersion, the transverse envelope equations become a useful tool to study the transverse collective motion in synchrotrons. During bunch compression, both space charge and its effect on dispersion are increasing. Therefore, the transverse envelope equation should be coupled with the longitudinal equation to give a full description of the beam dynamics of bunch compression. The coupled longitudinal-transverse set of equations takes the form

$$\begin{aligned} z_m'' + \left(\kappa_{z0} z_m - \frac{K_L}{z_m^3} \right) z_m - \frac{\varepsilon_z^2}{z_m^3} &= 0, \\ \sigma_x'' + \left[\kappa_{x0} - \frac{K_{sc}}{2X(X+Y)} \right] \sigma_x - \frac{\varepsilon_{dx}^2}{\sigma_x^3} &= 0, \\ \sigma_y'' + \left[\kappa_{y0} - \frac{K_{sc}}{2Y(X+Y)} \right] \sigma_y - \frac{\varepsilon_{dy}^2}{\sigma_y^3} &= 0, \\ D_x'' + \left[\kappa_{x0} - \frac{K_{sc}}{2X(X+Y)} \right] D_x &= \frac{1}{\rho(s)}, \end{aligned} \quad (1)$$

with the coupled relations

$$X = \sqrt{\sigma_x^2 + \sigma_\delta^2} D_x, \quad Y = \sigma_y, \quad (2)$$

and

$$\sigma_\delta = \sqrt{\left(\frac{\sigma_z'}{\eta} \right)^2 + \left(\frac{\varepsilon_z}{\eta \sigma_z} \right)^2}, \quad \sigma_z = \sqrt{5} z_m. \quad (3)$$

Here, $\kappa_{x0,y0}$ and κ_{z0} are the linearized external focusing gradients in transverse and longitudinal plane, respectively. $\sigma_{x,y}$ denote the transverse rms betatron beam size; X and Y the transverse rms total beam size with dispersion; σ_δ the rms momentum spread; σ_z the rms half bunch length; $\varepsilon_{dx,dy}$ the generalized transverse rms emittance defined in Ref. [5], and ε_z the longitudinal rms emittance.

PIC Simulations

A major consideration of PIC-simulation of bunch compression is the treatment of space charge. For typical parameters of bunch compression in synchrotrons, the bunch length after bunch compression is much larger than the transverse beam size. Therefore, the treatment of space charge in the

simulation can be split into a 1-D longitudinal calculation and a 2-D transverse calculation, which is often referred to as “2.5-D” in literature. Another consideration is the generation of the initial particle distribution. The longitudinal one can be chosen as parabolic, which is - at least initially - a self-consistent model. In order to compare with the envelope approach, the external longitudinal rf focusing force is chosen to be linear. In the transverse plane, the initial distribution is chosen as a Gaussian (truncated at 3σ , here σ is the standard deviation).

BUNCH COMPRESSION IN THE SIS-18

The lattice of the SIS-18 consists of 12 FODO cells. The related parameters for bunch compression are listed in Table 1 [6].

Table 1: Main Parameters for an Example Bunch Compression in SIS-18

| Parameters [unit] | Symbol | Value |
|--------------------------------|---------------------|--------------------|
| Circumference [m] | L | 216 |
| Slip factor | η | -0.5 |
| Bare tune | $Q_{0,x,y}$ | 4.27, 3.47 |
| Initial half bunch length [ns] | τ_i | 395 |
| Initial rms momentum spread | $\sigma_{\delta,i}$ | 5×10^{-4} |
| Final half bunch length [ns] | τ_f | 30.0 |
| RF voltage [kV] | V_{rf} | 33.7 |
| Required turns | n | 77 |
| rms emittance [mm mrad] | $\epsilon_{x,y}$ | 15, 5 |
| Periodic phase advance [deg] | $k_{0x,0y}$ | 128, 104 |

The results can be obtained from PIC simulation and the coupled-envelope equations. In longitudinal plane, the evolution of bunch length during bunch compression obtained from the coupled envelope equation is almost perfect matched with the simulation results (figure not shown here).

In transverse, Figure 1 shows the transverse results from the two approaches. The blue solid line and blue dotted line are the transverse rms beam size (X) and betatron rms beam size (σ_x) solved from the coupled envelope method. The red solid line and red dotted line are the transverse rms beam size and betatron rms beam size obtained from the simulation. It can be seen from Fig. 1 that during bunch compression the total horizontal beam size X is increasing due to the increasing dispersion, while the betatron beam size σ_x remains constant. The results of transverse beam sizes from the envelope approach agree well with the results from PIC simulations.

ENHANCED SPACE CHARGE EFFECTS DURING BUNCH COMPRESSION

90° -Fourth Order Particle Resonance

It is well-known that the envelope instability and a fourth-order resonance both driven by space charge are two major

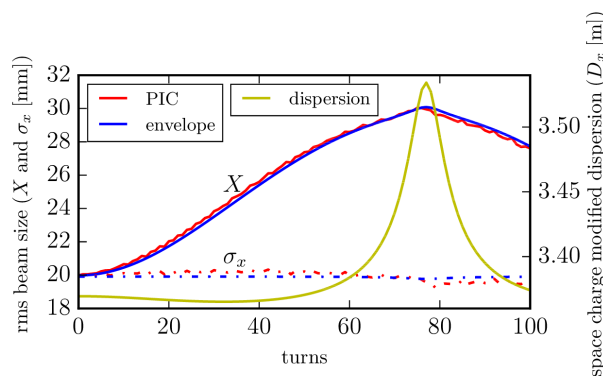


Figure 1: Evolution of the total rms beam size X , the betatron beam size σ_x and the space-charge-modified dispersion D_x during bunch compression obtained from PIC simulation and envelope approach.

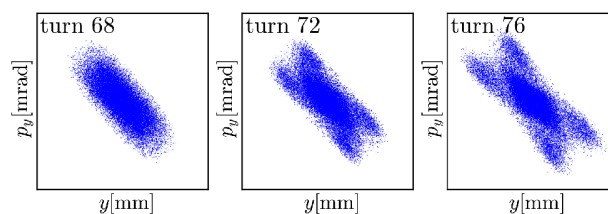


Figure 2: The evolution of particle distribution in the $y - y'$ phase space at final stage of bunch compression with double beam intensity at 68th, 72nd, 76th turns during bunch compression.

contributions for space charge limits in high intense beams, with the stop bands related to 90° phase advance per focusing period [7, 8].

Particle distributions in $y - p_y$ phase space at three representative turns (68th, 72nd, 76th) in final stage of bunch compression with doubled beam intensity are shown in Fig. 2. One can see a clear fourfold structure in $y - p_y$ phase space, characterizing the fourth-order resonance, with the condition

$$4\hat{k}_y = 360^\circ, \quad (4)$$

and no envelope instability is observed in PIC simulations. In other words, during bunch compression, the fourth order particle resonance dominates over the envelope instability. To illustrate the mechanism, we plot the comparison on location of phase advances to the phase shifts of envelope modes $\varphi_{1,2}$ and the coherent space charge tune shift $\Delta k_{\text{coh},y}$ obtained from envelope approach, as shown in Fig. 3. The criteria of envelope instability can be described as [3]

$$\varphi_2 = 2k_{0,y} - \Delta k_{\text{coh},y} = \frac{1}{2}360^\circ. \quad (5)$$

During bunch compression, with space charge increasing, all quantities except $k_{0,y}$ in Fig. 3 will decrease and dynamically move towards the 90° line. Clearly, the most depressed phase advance \hat{k}_y will firstly arrive at the 90° line,

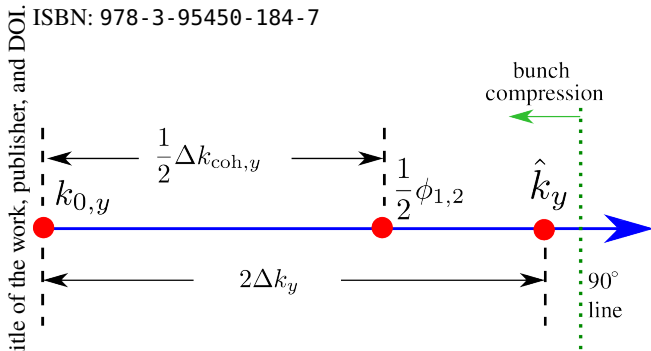


Figure 3: Schematic drawing of the comparison on location of the phase advances to the phase shifts of envelope modes $\varphi_{1,2}$. Dashed line denotes the 90° phase advance line during bunch compression.

and trigger the fourth-order resonance before $\frac{1}{2}\varphi_2$ arrives at the 90° line. The resulting emittance growth can weaken the space charge effect and prevent $\frac{1}{2}\varphi_2$ to approach the 90° resonance line, leading to the fourth-order resonance and prevent inducing the envelope instability.

120°-Dispersion Beam Instability

During bunch compression space charge as well as dispersion are increasing. With sufficiently high beam intensity and designed horizontal phase advance $k_{0,x}$ larger than 120° , as is the case for SIS-18, the combined effects of space charge and dispersion could induce the 120° dispersion instability, which is another limitation factor for bunch compression. In order to investigate this, we adjust $k_{0,x}$ from 128° to 122° in Tab. 1 and keep other parameters unchanged. By doing this, the horizontal phase advance k_x will cross the 120° line during bunch compression.

Particle distributions in $x - p_x$ phase space at three representative turns (72nd, 74th, and 76th) in the final stage of bunch compression are shown in Fig. 4, from which one can see the emittance deformation and the effect of emittance growth. We attribute the sharp emittance in Fig. 4 to the 120° dispersion instability, which is a collective effect with,

$$\varphi_1 + \varphi_d = 360^\circ, \quad (6)$$

when

$$k_{0,x} > 120^\circ \quad \text{and} \quad k_x < 120^\circ. \quad (7)$$

In order to further study the mechanism of intensity limitation related to the 120° dispersion instability, we calculate the fast mode φ_1 , slow mode φ_2 and dispersion mode φ_d with $k_{0,x} = 122^\circ$, $k_{0,y} = 104^\circ$. As shown in Fig. 5, with space charge increasing during bunch compression, the curve φ_d will be confluent with $360^\circ - \varphi_1$, indicating the dispersion-instability, which is in good agreement with the emittance deformation and growth at turn 74 in Fig. 4.

The onset of the dispersion-induced instability is not inhibited compared with that of the envelope instability. Firstly, compared with the competition between fourth-order resonance and envelope instability related to 90° , there is no obvious single particle resonance, which exists earlier and

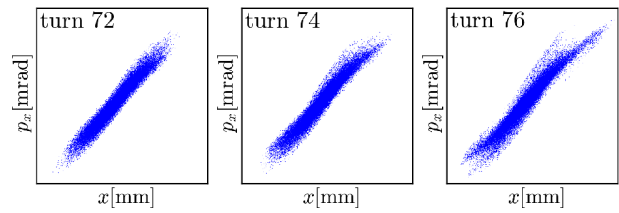


Figure 4: The evolution of particle distribution in the $x - x'$ phase space at final stage of bunch compression with $k_{0,x} = 122^\circ$, $k_{0,y} = 104^\circ$ at 72th, 74th, 76th turns during bunch compression.

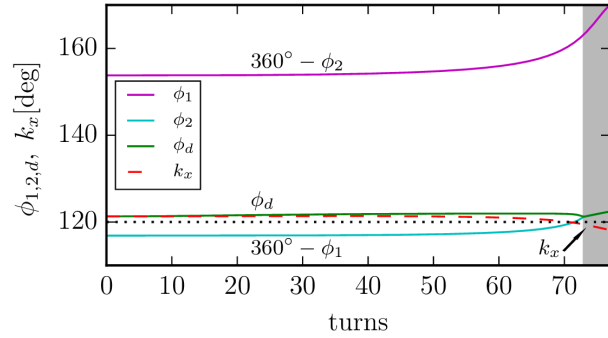


Figure 5: Phase shifts of the envelope modes φ_1 , φ_2 and dispersion mode φ_d numerically solved from the coupled envelope approach during bunch compression with $k_{0,x} = 122^\circ$ and $k_{0,y} = 104^\circ$. (Shaded area denotes the stop band of the dispersion-induced instability.)

can weaken the space charge and prevent the 120° dispersion instability. This is different from the case of the 90° envelope instability, which is suppressed by the competition with the fourth-order resonance. Secondly, the beam intensity threshold of 120° dispersion instability is much lower than that of 90° envelope instability, as can be seen in the Fig. 2 in Ref. [3]. Therefore, the former instability would need less time to develop than the latter.

CONCLUSION

The coupled longitudinal-transverse envelope equations including dispersion are applied to the bunch compression in SIS-18. The numerical results are found to agree well with PIC simulation results. Results show two major intensity limitations caused by space charge during bunch compression when phase advances dynamically cross 90° or 120° . When crossing 90° , the fourth-order resonance dominates over the envelope instability and leads to emittance growth. When crossing 120° , simulation results show that the recently discovered dispersion-induced instability could be another intensity limitation for bunch compression. The agreement between numerical envelope solutions and simulation results shows that the coupled longitudinal-transverse envelope approach defines the stop band of the 120° dispersion instability which should be avoided during bunch compression.

ACKNOWLEDGEMENT

One of the authors (Y. S. Yuan) was supported through a grant from HGS-HIRe for FAIR.

REFERENCES

- [1] <http://www.fair-center.eu/>
- [2] J. Struckmeier and M. Reiser, "Theoretical studies of envelope oscillations and instabilities of mismatched intense charged-particle beams in periodic focusing channels", *Part. Accel.* 14, 227 (1984).
- [3] Y. S. Yuan, O. Boine-Frankenheim, G. Franchetti and I. Hofmann, "Dispersion-Induced Beam Instability in Circular Accelerators", *Phys. Rev. Lett.* 118, 154801 (2017).
- [4] D. Neuffer, "Longitudinal Motion in High Current Ion Beams - A Self-Consistent Phase Space Distribution with an Envelope Equation", *IEEE Trans. Nucl. Sci.* 26, 3031 (1979).
- [5] M. Venturini and M. Reiser, "rms Envelope Equations in the Presence of Space Charge and Dispersion", *Phys. Rev. Lett.* 81, 96 (1998).
- [6] Oleksandr Chorniy *et al.*, "Fast Compression of Intense Heavy-Ion Bunches in SIS-18", *Proceedings of HB2010*, Morschach, Switzerland, 2010, p.686-689.
- [7] D. Jeon, L. Groening, and G. Franchetti, "Fourth order resonance of a high intensity linear accelerator", *Phys. Rev. ST Accel. Beams* 12, 054204 (2009).
- [8] I. Hofmann and O. Boine-Frankenheim, "Space-Charge Structural Instabilities and Resonances in High-Intensity Beams", *Phys. Rev. Lett.* **115**, 204802 (2015).